J Mater Sci (2008) 43:1723–1729
DOI 10.1007/s10853-007-2244-z

Modifier ligands effects on the synthesized TiO_2 nanocrystals

Abbas Sadeghzadeh Attar · Morteza Sasani Ghamsari · Fereshteh Hajiesmaeilbaigi · Shamsoddin Mirdamadi

Received: 29 November 2006 / Accepted: 22 October 2007 / Published online: 25 December 2007

Abstract In this study, the preparation of titanium dioxide nanocrystals by sol–gel method has been considered. Then, the effect of modifier ligands such as acetylacetone (AcAc) and acetic acid (AcOH) on synthesis of TiO_2 nanocrystalline powders has been investigated. The experimental results showed that the reaction of tetraisopropoxide titanium, $Ti(OPr^i)_4$, with acetylacetone and acetic acid leads to formation of complexes that can prevent the precipitation of undesired phases from highly reactive precursors. Whereas, the band of ligands to TiO_2 nanocrystals is not broken easily at temperatures lower than about 400 °C. So these ligands may remain in the final TiO_2 nanostructures and affect the morphology and structure of prepared materials. The studied samples were characterized using Fourier transform infrared spectroscopy (FT-IR), Thermogravimetric and Differential thermal analysis (TG-DTA), X-ray diffraction (XRD) and scanning electron microscopy (SEM).

Introduction

The structure and unique properties of TiO_2 nanostructures due to the specific surface area and quantum size effects can lead to important applications in photoelectrochemical, photocatalyst, dye-sensitized solar cell, gas sensor, and so on [1–8]. In order to prepare of TiO_2 nanostructures with significant properties, several processes have been developed over the last decade and can be classified as vapour (chemical vapour deposition [9–13], physical vapour deposition [14], spray pyrolysis deposition [15, 16]), liquid (sol–gel [17–23], solvothermal [24, 25], coprecipitation [26, 27], hydrothermal [28, 29]), solid state processing routes (mechanical alloying/milling [30–32], mechanochemical [33]), and other routes such as laser ablation [34], RF thermal plasma [35]. From mentioned methods, the sol–gel process is very promising for synthesis and preparation inorganic and organic–inorganic hybrid nanomaterials which allow low processing temperatures (typically <100 °C) and molecular level composition homogeneity. It is based on hydrolysis and condensation reactions of molecular precursors such as metal alkoxides ($M(OR)_n$, M = Ti, Zr, Si, ...) and inorganic salts [36–39]. Metal alkoxides which are used as precursor materials for sol–gel process are generally highly reactive species. Thus control of the reactivity of metal alkoxides is necessary in order to obtain sols and gels with desirable properties. This control may be achieved through the addition of "modifiers" such as β-diketones (e.g., acetylacetone), carboxylic acids (e.g., acetic acid) or other complex ligands. They chemically react with alkoxides at a molecular level and giving rise to new molecular precursors. Such modified alkoxide precursors can be used in sol–gel processing for a better control of the hydrolysis-condensation process [39–49]. Acetylacetone is known to be a rather strong chelating ligand; it is often used as a stabilizing agent for non-silicate alkoxides precursors. The enolic form of acetylacetone contains a reactive hydroxyl group which reacts readily with metal alkoxides and results in the transfer of an acidic

A. S. Attar · S. Mirdamadi
Department of Metallurgy and Materials Engineering,
Iran University of Science and Technology, Tehran, Iran

S. Mirdamadi
e-mail: mirdamadi@iust.ac.ir

M. S. Ghamsari (✉)
Solid State Lasers Research Group, Laser and Optics Research School, NSTRI, Tehran 11365-8486, Iran
e-mail: msghamsari@yahoo.com

F. Hajiesmaeilbaigi
Solid State Lasers Research Group, Laser Research Center,
Tehran 11365-8486, Iran

proton from the acetylacetone to an alkoxy ligand, yielding the corresponding alcohol and a modified alkoxide precursor as follows [49–51]:

$$Ti(OPr^i)_4 + x(acacH) \rightarrow Ti(OPr^i)_{4-x}(acac)_x + xPr^iOH \tag{1}$$

In this reaction, the reactive noncomplex precursors ($Ti(OPr^i)_4$) is in equilibrium with the less reactive modified metal alkoxides ($Ti(OPr^i)_{4-x}(acac)_x$). The concentration of the different species depends on the nature of the metal atom and the initial complex ratio [40].

Acetic acid is another popular modifier that it can easily dissolve a wide variety of different precursor molecules, helping to create a multitude of multi-cation solutions. Precipitation readily occurs when water is added to $Ti(OPr^i)_4$, while homogeneous and clear transparent TiO_2 gels are obtained in the presence of acetic acid. When acetic acid is added to Ti alkoxides, an exothermic reaction takes place which leads to a new molecular precursor:

$$Ti(OPr^i)_4 + AcOH \rightarrow Ti(OPr^i)_3(OAc) + Pr^iOH \tag{2}$$

Birnie and coworker [52, 53] have shown these chemistries are sometimes touchy because the acetic acid can drive an esterification reaction with any alcohol that is present, thus this reaction leads to liberating of the water in the solution. The esterification reaction can present some potential problems for sol–gel routes. As the reaction is not controlled, the liberated water can cause precursor condensation reactions (and ultimately precipitation) in the solution [52, 53]. However, the presence of these modifier materials will be useful for controlling the hydrolysis and condensation reactions and prevent the precipitation of undesired phases. But, these ligands remain in TiO_2 nanostructures at temperatures lower than about 400 °C and may affect the final properties of TiO_2. It seems that there are no enough research results about the remaining of these ligands in prepared TiO_2 nanopowders. Thus, a good understanding of chemical principles and their effects on structure of TiO_2 nanocrystals is necessary.

In the present work, a study on the preparation of TiO_2 nanocrystals with acetylacetone and acetic acid has been considered. Then the presence of these modifier ligands in the prepared TiO_2-sols, as-prepared powders, and annealed powders at 300, 400, and 500 °C has been investigated by Fourier transform infrared spectroscopy (FT-IR), Thermogravimetric and Differential thermal analysis (TG-DTA), X-ray diffraction (XRD), and scanning electron microscopy (SEM).

Experimental

The TiO_2 nanocrystalline powders were synthesized by sol–gel process and followed by drying and heat treatment processes. The TiO_2-sols were prepared by using two modifiers and without modifier. In the first approach, the acetylacetone was added into the prepared solution. The TiO_2-sol was formed by mixing of titanium tetraisopropoxide (TTIP; Merck, ≥98%), acetylacetone (Merck, ≥99.5%), deionized water, and ethyl alcohol (Merck, ≥99.8%). At first, 5 mmol acetylacetone was mixed with 5 mmol of TTIP by using magnetic stirring. This reaction was exothermic and resulted in a yellow solution, while both precursors were colorless liquids. Then the new resulted precursor was diluted in 25 mL of ethanol. At last, 25 mL of water was added to the solution with an automatic stirring in 2 h. This colloidal solution remained stable over several months.

In the second approach, the TiO_2-sol was prepared in the presence of acetic acid. TiO_2-sol was formed by dissolving TTIP in glacial acetic acid and stirring for 30 min at room temperature. Then deionized water was added to the solution and a white precipitate was instantaneously formed. However, the sol became a clear liquid after about 5 min of stirring. In this method, the molar ratio of the TTIP: AcOH: H_2O was 1:10:17.

For the preparation of TiO_2-sol without modifier, 1.47 mL of TTIP was added slowly to a mixture of 25 mL H_2O, 25 mL EtOH, and HNO_3 under vigorous stirring at 60–70 °C for 20 h.

After drying of TiO_2-sols in the air at room temperature for 24 h, the prepared specimens were put into a muffle furnace and then were heat-treated as per the procedure. At the first step, the samples were held at 100 °C for 8–10 h to remove the residual water completely. In the next step, they were heated up to 300, 400, and 500 °C at a rate of 2.5 °C/min and held for 2 h. At last, the furnace was shut down and the samples were cooled back to room temperature naturally.

The FT-IR spectra were recorded at room temperature with a Bruker (Vector 22 model) spectrophotometer in the range of 400–4,000 cm^{-1}. Thermal analysis of the samples were carried out using TG/DTA Rheometric Scientific STA 1500 spectrometer in air at a heating rate of 10 °C/min. The XRD patterns of TiO_2 nanocrystalline powders were collected with a Philips PW 1800 diffractometer using filtered monochromatized Cu Kα radiation ($\lambda = 1.54056°A$) to determine crystal size and phase structures. The size and morphology of TiO_2 nanopowders were characterized by scanning electron microscopy (CamScan MV2300).

Results and discussion

The FT-IR spectra of the TiO_2-sols, as-prepared powders and annealed powders at 300, 400, and 500 °C in the presence of AcAc, AcOH, and without modifier have been illustrated in Figs. 1–3. The FT-IR spectrum recorded on

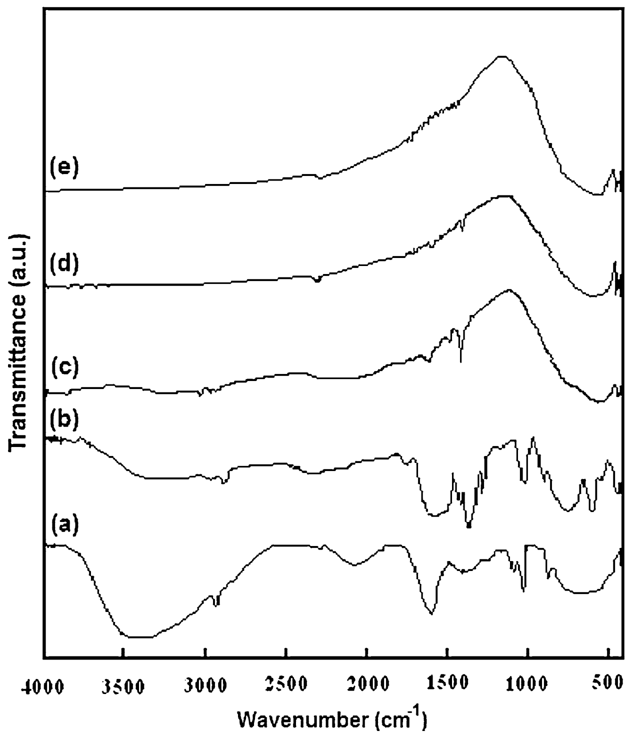

Fig. 1 FT-IR spectra of the TiO_2 nanostructures modified by AcAc (**a**) sol (**b**) as-prepared powder and annealed powders at (**c**) 300 °C (**d**) 400 °C (**e**) 500 °C

the TiO_2-sol with AcAc (Fig. 1a) shows one peak at 3,410 cm^{-1}, which assigned to νOH stretching of Ti–OH. No bands appear around 1,700 cm^{-1} which can be attributed to ν(C=O) vibration of free acetylacetone. Apparently, the acetylacetone has been completely consumed in the reaction. Infrared spectrum clearly exhibits bands at 1,590 cm^{-1} (ν (C=O) + ν (C=C)), 1,450 cm^{-1} (δ (CH_3)), and 1,080 cm^{-1} (ρ (CH_3)) due to acetylacetanato groups which are bound to titanium. The bands at 1,040 and 875 cm^{-1} are due to free ethanol, while the other broad bands below 900 cm^{-1} are characteristic of a Ti–O–Ti network. It seems that the presence of these bands can be explained by the chemical reactions between acetylacetone and Ti alkoxide. All the AcAc ligands in solution can not be removed even in the presence of a large excess of water. Therefore, the colloidal nanoparticles in TiO_2-sol can be described as anatase TiO_2 particles with acetylacetonato groups bound to Ti surface sites. Infrared spectrum of the as-prepared powder (Fig. 1b) indicates that there are several bands around 1,570, 1,420, and 1,270 cm^{-1} which can be attributed to the remaining acetylacetonato groups bound to titanium. Often these bands disappear when the powder is heated to high temperatures. After annealing at 300 °C (Fig. 1c), peaks attributed to adsorbed water almost disappeared, while the vibration of the hydroxyl groups could be still observed at about 3,140 cm^{-1}. Also, it can be found that bands are still at 1,580, 1,480, and 1,415 cm^{-1} which are relative to acetylacetanato groups. The appearance of new bands around 490, 425 cm^{-1} and 485, 410 cm^{-1} can be seen at 400 and 500 °C, respectively (Fig. 1d, e). We have assigned these bands to the ν Ti–O–Ti stretching vibration in the anatase phase. After annealing at 400 °C, the residuals were peaks only for Ti–O vibration located at 400–700 cm^{-1}.

Figure 2 shows the infrared spectra of the TiO_2-sol and TiO_2 nanopowders in the presence of AcOH. Characteristic vibrations of acetate groups bonded Ti (ν_c COO at 1,410 cm^{-1} and ν_{as} COO at 1,630, 1,520 cm^{-1}) are observed in Fig. 2a. Vibrations due to acetic acid (ν C=O at 1,720 cm^{-1}) and remaining ester (ν C=O at 1,765, 1,785, 1,240, and 1,170 cm^{-1}) show that a few of the AcOH ligands are still adsorbed in the precipitations. The bands around 1,740, 1,525, and 1,430 cm^{-1} in the uncalcinated samples (Fig. 2b) show that some of the acetate groups are still remaining in the compound. These compounds exhibit broad bands from 900 cm^{-1} to 400 cm^{-1} characteristic of the ν Ti–O–Ti vibration of TiO_2 network. After annealing at 300 °C (Fig. 2c), the bands around 1,200–1,700 cm^{-1} show that acetate groups remain in TiO_2 powders and have not been broken completely. The spectra of annealed TiO_2 at 400 and 500 °C (Fig. 2d, e) show the bands around 650,

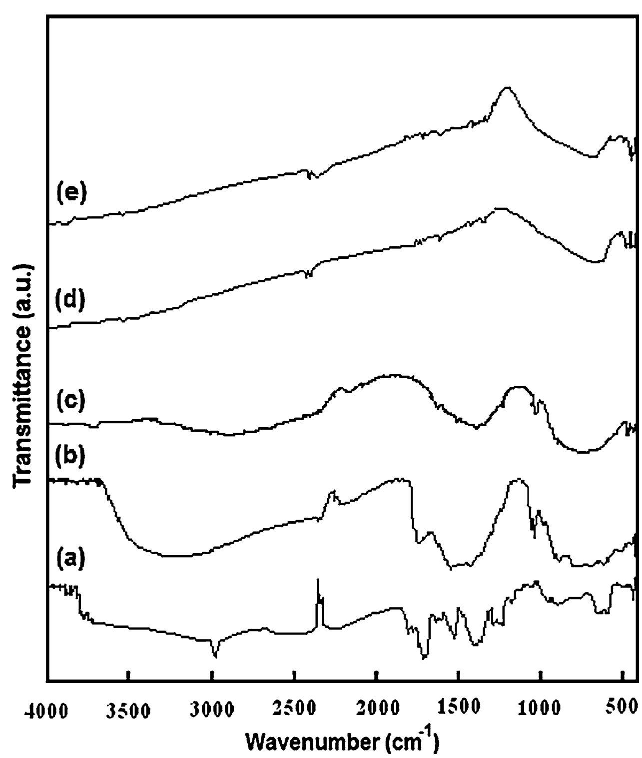

Fig. 2 FT-IR spectra of the TiO_2 nanostructures modified by AcOH (**a**) sol (**b**) as-prepared powder and annealed powders at (**c**) 300 °C (**d**) 400 °C (**e**) 500 °C

410 cm^{-1} and 655, 415 cm^{-1} that are attributed to Ti–O–Ti network. Limmer et al. [54] have shown only acetylacetone remains strongly bound to the Ti species and affect the final TiO_2 nanostructures. But the FT-IR results in this work show the both of AcAc- and AcOH-modifier ligands bind strongly to precursors and complex species remain bound to titanium. The crystallization of the pure TiO_2 anatase phase occurs above 400 °C in the presence of acetylacetone and acetic acid.

The FT-IR spectra of the prepared TiO_2-sol and nanopowders without nucleophilic ligands have been shown in Fig. 3. The broad adsorption peak near 3,400 cm^{-1} (Fig. 3 a) is related to stretching vibration of Ti–OH groups. On other hand, the peak at 1,620 cm^{-1} is assigned to bending vibration of coordinated water. It can be seen in Fig. 3b that organic groups such as ethyl and isopropyl groups are still present in the as-prepared powder. In the powders heated to 300 °C (Fig. 3c), all these bands disappeared showing that the organic materials were completely removed from the nanopowders. The 430 cm^{-1} "anatase" band is first seen (Fig. 3c) at a temperature of about 300 °C. The Ti–O peaks, due to the presence of nucleophilic ligands bound to Ti were weak in Figs. 1c and 2c. The intensity of Ti–O bands is found to increase as the powders were further heated at 400 and 500 °C (Fig. 3d, e).

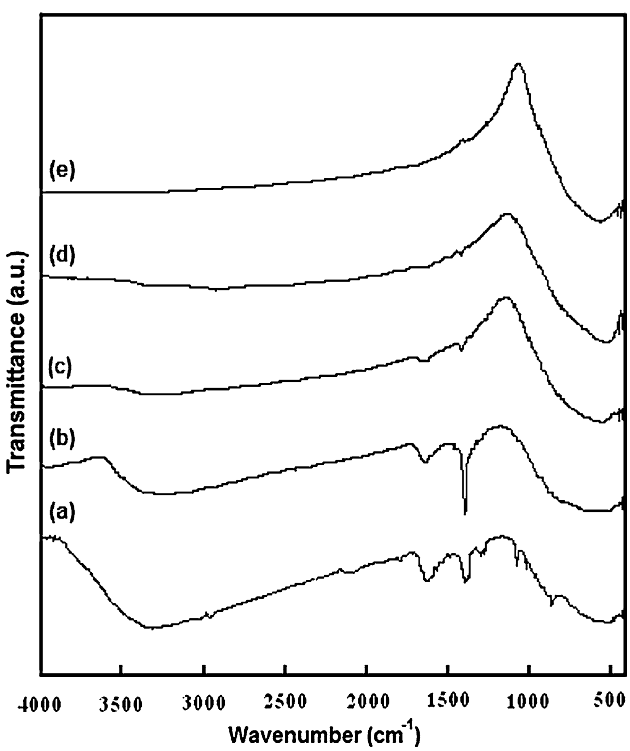

Fig. 3 FT-IR spectra of the TiO_2 nanostructures without modifier (**a**) sol (**b**) as-prepared powder and annealed powders at (**c**) 300 °C (**d**) 400 °C (**e**) 500 °C

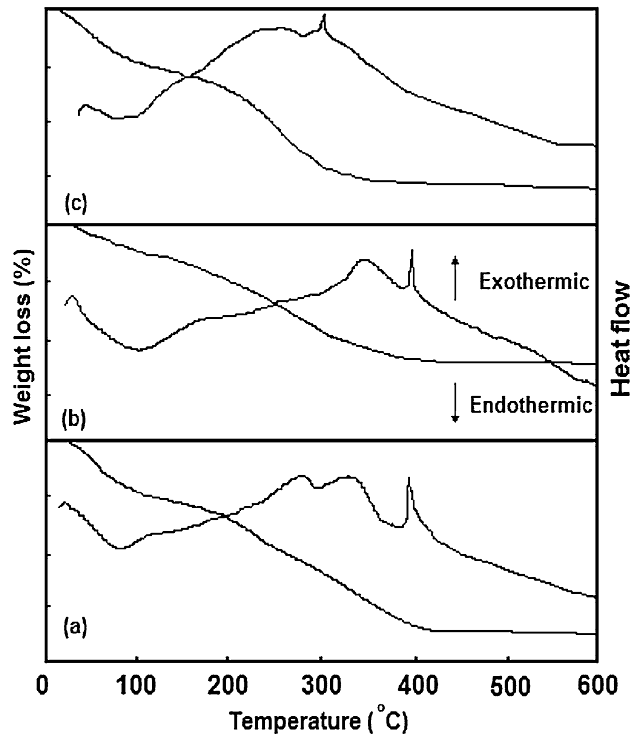

Fig. 4 TG-DTA curves of (**a**) AcAc-modified TiO_2 (**b**) AcOH-modified TiO_2 (**c**) without modifier

The thermal behavior of TiO_2 nanoparticles have been investigated with a TG-DTA technique at temperatures ranging from room temperature to 600 °C and the TG-DTA pattern of the typical TiO_2, nanoparticles have been shown in Fig. 4. At all the TG-DTA curves, the endothermic peaks and the sample weight loss at below 120 °C are attributed to the removal of physically water and solvent. The exothermic peak at about 270 °C and a broad exothermic peak at 300–400 °C (Fig. 4a) are due to the combustion of organic compounds, residual hydroxyl groups, and acetyacetanate ligands. There is a peak at 360 °C in the Fig. 4b that is corresponded to the decomposition of acetate ligands. At 385 °C the observed exothermic peak is attributed to the crystallization of the amorphous phase into the anatase phase. This peak appears at 390 and 305 °C for the samples with AcOH ligands and without ligands. Above 400 °C, it can be assumed that the product completely transforms into crystalline phase, because there is no change in particle weight. Two mass losses can be observed on TG curves. The first weight loss corresponds to the departure of free water about 12% (for AcAc), 7% (for AcOH), and 13% (for without ligand) in range 80–120 °C. In the range of 220–400 °C, there is second weight loss of about 22%, 15%, and 17% for samples of with AcAc, AcOH, and without ligand, respectively. However, for prepared samples with AcAc and without ligand weight loss, it is obviously more than

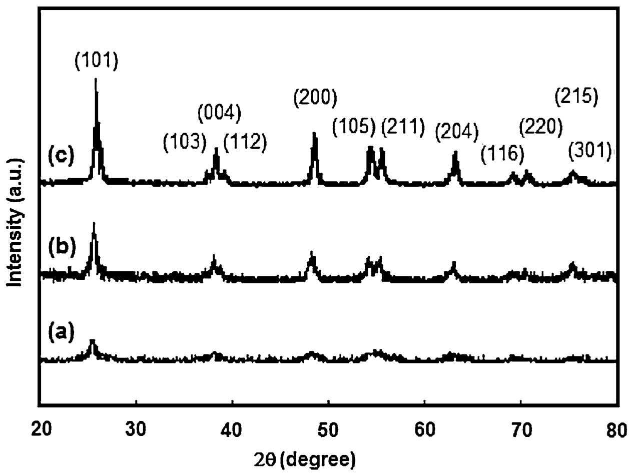

Fig. 5 XRD pattern of the prepared TiO_2 nanopowders by AcAc, annealed at (**a**) 300 °C (**b**) 400 °C and (**c**) 500 °C

that of the AcOH due to a large amount of water and ethanol.

Figures 5–7 show the XRD spectra of the TiO_2 nanopowders annealed at 300, 400, and 500 °C for 2 h. The peak positions and their relative intensities in all samples are consistent with the standard powder diffraction pattern of pure anatase phase. Comparison of the XRD patterns shows that there are identical peaks in all the TiO_2 nanoparticles. The crystallite size of these samples was estimated using the Scherrer's equation [55]:

$$D = \frac{0.9\lambda}{\beta\cos\theta} \quad (3)$$

where λ is the X-ray wavelength, β is the full-width at half-maximum intensity (FWHM). The broadening of TiO_2 peaks show that the crystallite size is small. The average crystallite size for obtained TiO_2 nanoparticles in the presence of AcAc increases from 20 nm to 30 nm with increasing annealing temperature from 400 °C to 500 °C. In addition, with increasing annealing temperature from 300 °C to 500 °C, the peak intensities and crystallity of anatase increase and width of the (101) diffraction peak of anatase ($2\theta = 25.4°$) becomes narrower. These measurements have shown that the nanoparticles heated at temperatures lower than 400 °C are not crystalline in prepared nanopowders with AcAc and AcOH. But TiO_2 nanoparticles without complex ligands are crystalline at 300 °C (Fig. 7). In the presence of complex ligands, the phase transformation temperature of amorphous to anatase increases. These compounds prevent crystallization of TiO_2 nanopowders at temperature lower than 400 °C.

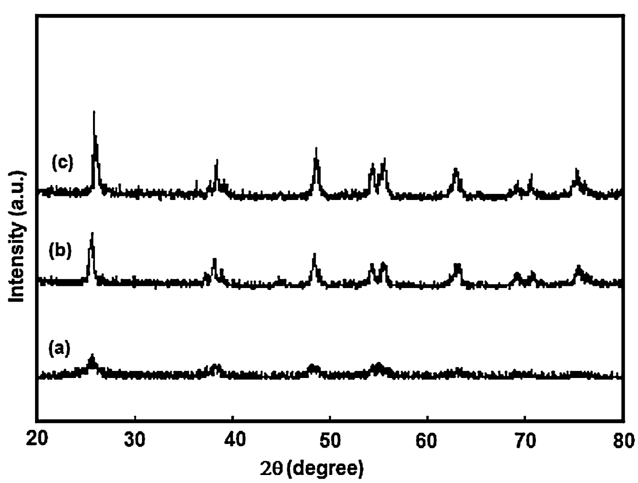

Fig. 6 XRD pattern of the prepared TiO_2 nanopowders by AcOH, annealed at (**a**) 300 °C (**b**) 400 °C and (**c**) 500 °C

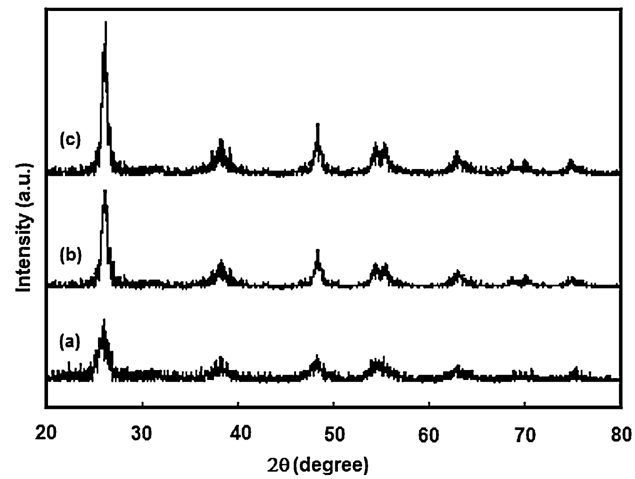

Fig. 7 XRD pattern of the prepared TiO_2 nanopowders without modifier, annealed at (**a**) 300 °C (**b**) 400 °C and (**c**) 500 °C

The SEM images of the prepared TiO_2 nanoparticles with AcAc, AcOH, and without modifier have been shown in Figs. 8–11, respectively. At 400 °C, the micrographs (Figs. 8, 9) show that the nanoparticles have a spherical and narrow size distribution with a very small particle size about 20–25 nm for AcAc and 25–30 nm for AcOH. The size of TiO_2 nanoparticles increases to 30 nm for sample prepared by acetylacetone (Fig. 10). For TiO_2 nanoparticles without complex ligands (Fig. 11), the precipitate particles are found to be highly agglomerated and some are nonspherical particles. These differences in morphology and particle size indicate that the presence of the nucleophilic ligands can produce fine and discrete sphere nanoparticles. The crystallite sizes calculated from XRD analysis are nearly the same as those obtained from SEM analysis.

Conclusion

The direct addition of water to titanium alkoxides generally leads to precipitate TiO_2 nanopowders. The stable TiO_2 sols can be prepared by using the acetylacetone and acetic

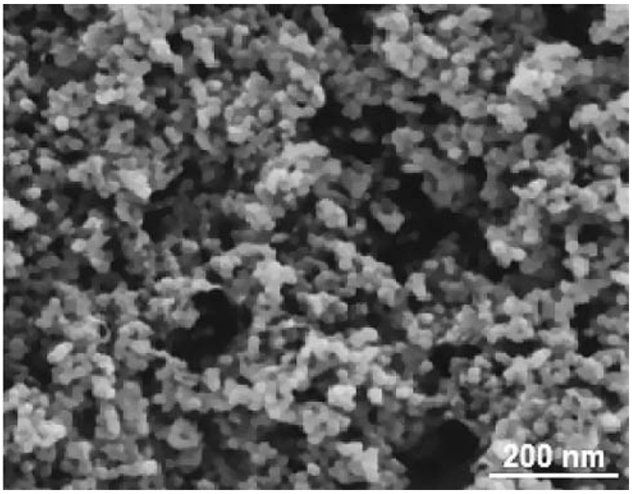

Fig. 8 SEM image of AcAc-modified TiO_2 nanopowders, annealed at 400 °C for 2 h

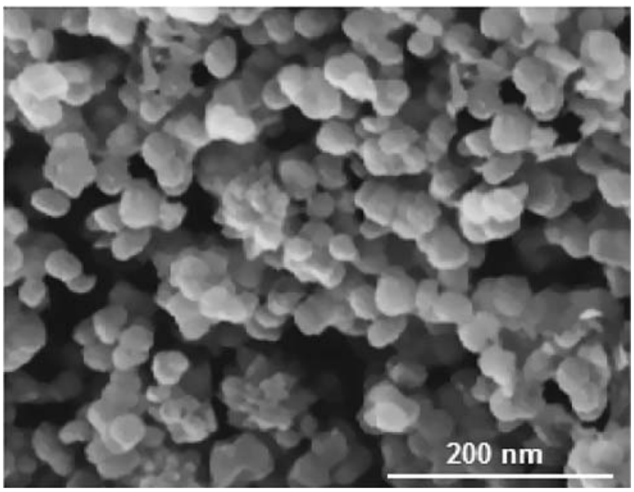

Fig. 9 SEM image of AcOH-modified TiO_2 nanopowders, annealed at 400 °C for 2 h

acid in chemical solution. The hydrolysis reaction in the presence of acetylacetone is incomplete and acetylacetonato groups still remain bound to Ti even when hydrolysis is performed with a large excess amount of water. Also, in the presence of acetic acid, acetate groups are not immediately removed through hydrolysis or condensation reactions. These complex compounds prevent crystallization and are present at temperatures lower than 400 °C. However, crystallization of the pure TiO_2 anatase phase is found to begin at temperature higher than 400 °C for nanocrystals prepared with acetylacetone and acetic acid.

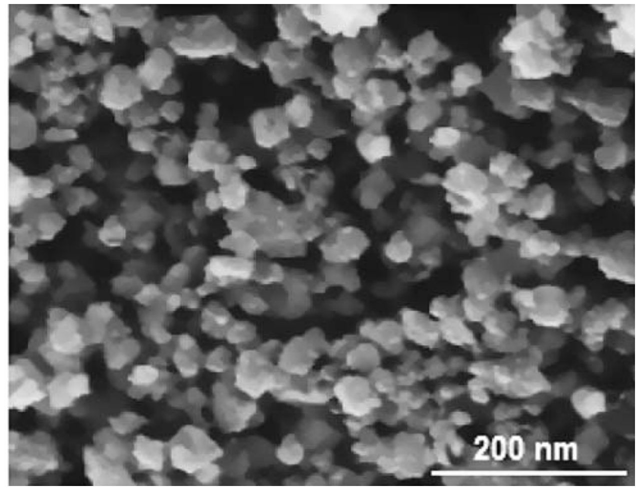

Fig. 10 SEM image of AcAc-modified TiO_2 nanopowders, annealed at 500 °C for 2 h

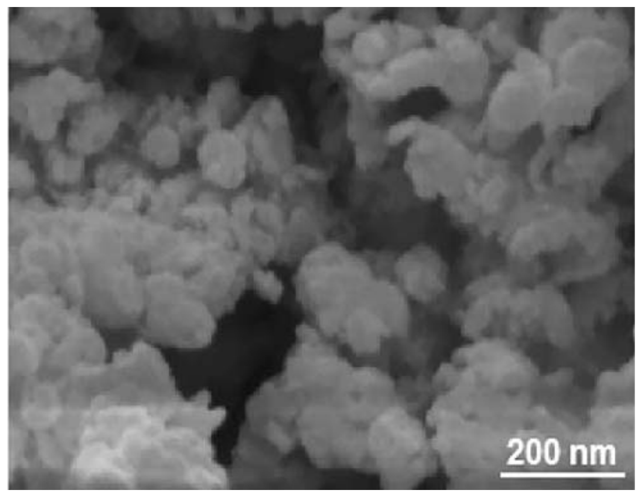

Fig. 11 SEM image of TiO_2 nanopowders, without modifier annealed at 400 °C for 2 h

References

1. Boujday S, Wunsch F, Portes P, Bocquet J-F, Colbeau-Justin C (2004) Sol Energ Mat Sol C 83:421
2. Kolen'ko YV, Churagulov BR, Kunst M, Mazerolles L, Colbeau-Justin C (2004) Appl Catal B Environ 54:51
3. Monticone S, Tufeu R, Kanaev AV, Scolan E, Sanchez C (2000) Appl Surf Sci 162–163:565
4. Tjong SC, Chen H (2004) Mater Sci Eng R 45:1
5. Jiu J, Isoda S, Wang F, Adachi M (2006) J Phys Chem B 110:2087
6. Carp O, Huisman CL, Reller A (2004) Prog Solid State Ch 32:33
7. Yu J, Wang G, Cheng B, Zhou M (2007) Appl Catal B Environ 69:171
8. Yu J, Su Y, Cheng B, Zhou M (2006) J Mol Catal A Chem 258:104
9. Kim B-H, Lee J-Y, Choa Y-H, Higuchi M, Mizutani N (2004) Mater Sci Eng B 107:289
10. Backman U, Auvinen A, Jokiniemi JK (2005) Surf Coat Technol 192:81
11. Wang K-H, Hsieh Y-H, Chao P-W, Cgang C-Y (2002) J Hazard Mater 95:161
12. Bessergenev VG, Khmelinskii IV, Pereira RJF, Krisuk VV, Turgambaeva AE, Igumenov IK (2002) Vacuum 64:275

13. Li W, Shah SI, Huang C-P, Jung O, Ni C (2002) Mater Sci Eng B 96:247
14. Bardos L, Barankova H (2001) Surf Coat Technol 146–147:463
15. Jokanovic V, Spasic AM, Uskokovic D (2004) J Colloid Interface Sci 278:342
16. Okuya M, Shiozaki K, Horikawa N, Kosugi T, Kumara GRA, Madarasz J, Kaneko S, Pokol G (2004) Solid State Ionics 172:527
17. Djaoued Y, Bruning R, Bersani D, Lottici PP, Badilescu S (2004) Mater Lett 58:2618
18. Trung T, Cho W-J, Ha C-S (2003) Mater Lett 57:2746
19. Sugimoto T, Zhou X, Muramatsu A (2003) J Colloid Interface Sci 259:53
20. Sugimoto T, Zhou X, Muramatsu A (2002) J Colloid Interface Sci 252:339
21. Sugimoto T, Zhou X, Muramatsu A (2002) J Colloid Interface Sci 252:347
22. Arnal P, Corriu RJP, Leclercq D, Mutin PH, Vioux A (1997) Chem Mater 9:694
23. Yu J, Yu JC, Hob W, Leung MKP, Cheng B, Zhang G, Zhao X (2003) Appl Catals A Gen 255:309
24. Kim C-S, Moon BK, Park J-H, Chung ST, Son S-M (2003) J Cryst Growth 254:405
25. Kim C-S, Moon BK, Park J-H, Choi B-C, Seo H-J (2003) J Cryst Growth 257:309
26. Xie Y, Yuan C (2004) Mater Res Bull 39:533
27. Palmisano L, Augugliaro V, Sclafani A, Schiavello M (1988) J Phys Chem 92:6710
28. Nian J-N, Teng H (2006) J Phys Chem B 110:4193
29. Ruiz AM, Sakai G, Cornet A, Shimanoe K, Morante JR, Yamazoe N (2004) Sens Actuators B Chem 103:312
30. Kim DH, Hong HS, Kim SJ, Song JS, Lee KS (2004) J Alloy Compd 375:259
31. Xiaoyan P, Xueming M (2004) Mater Lett 58:513
32. Guimaraes JL, Abbate M, Betim SB, Alves MCM (2003) J Alloy Compd 352:16
33. Kamei M, Mitsuhashi T (2000) Surf Sci 463:L609
34. Tsai M-H, Chen S-Y, Shen P (2005) Aerosol Sci 36:13
35. Oh S-M, Ishigaki T (2004) Thin Solid Films 457:186
36. Limmer SJ, Chou TP, Cao GZ (2004) J Mater Sci 39:895, doi:10.1023/B:JMSC.0000012919.21763.b2
37. Miao L, Tanemura S, Toh S, Kaneko K, Tanemura M (2004) J Cryst Growth 264:246
38. Steunou N, Ribot F, Boubekeur K, Maquet J, Sanchez C (1999) New J Chem 23:1079
39. Livage J, Henry M, Sanchez C (1988) Prog Solid State Ch 18:259
40. Scolan E, Sanchez C (1998) Chem Mater 10:3217
41. Doeuff S, Henry M, Sanchez C, Livage J (1987) J Non-Cryst Solids 89:206
42. Doeuff S, Henry M, Sanchez C (1990) Mat Res Bull 25:1519
43. Wu M, Lin G, Chen D, Wang G, He D, Feng S, Xu R (2002) Chem Mater 14:1974
44. Livage J, Henry M, Jolivet JP, Sanchez C (1990) MRS Bull XV:17
45. Ribot F, Toledano P, Sanchez C (1991) Chem Mater 3:759
46. Chatry M, Henry M, Livage J (1994) Mater Res Bull 29:517
47. Percy MJ, Bartlett JR, Woolfrey JL, Spiccia L, Westa BO (1999) J Mater Chem 9:499
48. Chatry M, Henry M, In M, Sanchez C, Livage J (1994) J Sol-gel Sci Techn 1:233
49. Sanchez C, Livage J, Henry M, Babonneau F (1988) J Non-Cryst Solids 100:65
50. Leaustic A, Babonneau F, Livage J (1989) Chem Mater 1:240
51. Leaustic A, Babonneau F, Livage J (1989) Chem Mater 1:248
52. Birnie DP (2000) J Mater Sci 35:367, doi:10.1023A:1004770007284
53. Birnie DP, Bendzko NJ (1999) Mater Chem Phys 59:26
54. Limmer SJ, Chou TP, Cao GZ (2005) J Sol-gel Sci Techn 36:183
55. Cullity BD (1978) Elements of X-ray Diffraction. Addison Wesley pub., Menlo Park